### Title

Recovery of Rare Earth Elements from Low-Grade Feedstock Leachates Using Engineered Bacteria




### Journal

Environmental Science and Technology, 51(22)

### ISSN

0013-936X



### Authors

Park, Dan M
Brewer, Aaron
Reed, David W
et al.



### Publication Date

2017-11-21

### DOI

10.1021/acs.est.7b02414

Peer reviewed

# Recovery of Rare Earth Elements from Low-Grade Feedstock Leachates Using Engineered Bacteria

Dan M. Park,[†] Aaron Brewer,[†,‡] David W. Reed,[§] Laura N. Lammers,[∥] and Yongqin Jiao*[,†]

[†]Physical and Life Science Directorate, Lawrence Livermore National Laboratory, Livermore, California 94550, United States
[‡]Univiersty of Washington, Earth and Space Sciences, Seattle, Washington 98195, United States
[§]Department of Biological and Chemical Processing, Idaho National Laboratory, Idaho Falls, Idaho 83415, United States
[∥]Department of Environmental Science, Policy, and Management, University of California, Berkeley, California 94720, United States

*Supporting Information*

ABSTRACT: The use of biomass for adsorption of rare earth elements (REEs) has been the subject of many recent investigations. However, REE adsorption b increase in distribution coefficients for individual REEs. Second, the relative affinity of the cell surface for REEs was increased over all non-REEs except Cu. T

## INTRODUCTION

Rare earth elements (REEs) are critical components of many clean energy technologies (e.g., wind turbines and hybrid car batteries) and consumer products (e.g., mobile phones, laptops, appliances, and automotive sensors).[1] As such, constraints or limitations in the supply of REEs could hinder the growth of technology industries that are critical for the transition to a low- carbon economy.[2,3] Greater than 90% of the global REE supply is obtained from China, leaving the global market vulnerable to supply restrictions as was observed recently when export quotas were tightened.[4] To alleviate supply vulnerability and diversify the global REE supply chain, it is imperative to develop new extraction methodologies and explore alternative REE resources.

Nontraditional REE resources, such as mine tailings, geothermal brines and coal byproducts are abundant and offer a potential means to diversify the REE supply chain.[5−8] However, given the low REE content and high concentrations

development of alternative technologies that enable efficient recovery of REEs from nontraditional feedstocks is highly desirable.

Microbially mediated surface adsorption (biosorption) represents a potentially cost-effective and ecofriendly approach for metal recovery.[12−15] Microorganisms exhibit high metal adsorption capacities because of their high surface area per unit weight and the abundance of cell surface functional groups (e.g., carboxylates and phosphates) with metal coordination functionality.[15] Additionally, the reversibility and fast kinetics of adsorption enable an efficient metal extraction process,[16−18] while the ability of cells to withstand multiple adsorption− desorption cycles avoids the need for frequent cell-regeneration,[17,19] decreasing operational costs. Biosorption is also expected to have a minimal environmental impact relative to traditional extraction techniques.[12,15]

Biosorption could be particularly well-suited for REE extraction given reports of selective adsorption of REEs over

of competing metals present in these feedstocks, conventional REE-extraction approaches are prohibitive at an industrial scale.[9] These REE extraction approaches, particularly hydrometallurgy via solvent extraction, are also energy intensive and pose severe environmental burdens.[10,11] Therefore, the



DOI: 10.1021/acs.est.7b02414
*Environ. Sci. Technol.* 2017, 51, 13471−13480

Received: May 17, 2017
Revised: September 22, 2017
Accepted: September 25, 2017
Published: September 25, 2017

non-REEs.[20−23] For example, $Tm^{3+}$ was preferentially adsorbed over $Fe^{2+}$ and $Mn^{2+}$ by *Bacillus subtilis*,[23] while $Sm^{3+}$ was adsorbed over $Cu^{2+}$, $Mn^{2+}$, $Co^{2+}$, $Ni^{2+}$, $Zn^{2+}$, and $Cd^{2+}$ by *Arthrobacter nicotianae*.[22] Additionally, the stability constant for the interaction of *B. subtilis* with $Nd^{3+}$ was stronger than for all other tested metal cations, except the uranyl oxycation.[21] Furthermore, despite the highly similar physicochemical properties of REEs, a general biosorption preference for heavy REEs over light REEs has been observed,[16,24,25] highlighting the potential of biosorption for enrichment of individual REEs. Indeed, a recent study reported a pH-dependent REE desorption scheme that achieved separation factors for certain REE pairs that exceeded solvent extraction standards.[26] Nevertheless, it remains an open question whether biosorption will be an effective means for selective extraction of REEs from low-grade feedstocks that contain high concen- trations of competing metals.

To further improve the adsorption capacity and selectivity of the cell surface for particular metals (e.g., Au and Pb), bioengineering approaches have been successfully used to display selective metal-binding peptides or proteins on the cell surface.[12,13,17,27−29] We recently reported the construction of a recombinant *Caulobacter crescentus* REE-adsorbing strain with lanthanide binding tags (LBT)[30] inserted at a permissive site of the S-layer protein, anchoring the LBT to the cell surface.[17] This approach enhanced the ability of *C. crescentus* to extract REEs from a high-grade REE ore leachate.[17] However, the concentrations of adsorbed non-REE metals were not quantified, precluding evaluation of the selectivity of REE adsorption. Furthermore, a maximum of eight copies of LBT per S-layer protein was achieved due to cellular toxicity, limiting the REE adsorption capacity of the *Caulobacter* system. In order to improve the REE adsorption capacity and adapt the LBT surface display to a broader range of microbial species, here we utilized the abundant surface protein OmpA[31,32] as an anchor for LBT display in *E. coli*. The resulting LBT-displayed strain was used directly as a whole cell adsorbent with feedstock leachates of complex matrix and low REE content. Our results demonstrate the feasibility of coupling bioengineering with biosorption for REE extraction from low-grade feedstocks.

## MATERIALS AND METHODS

**Construction of Plasmids for Surface Display of LBT in *E. coli*.** Multiple, adjacent copies of dLBT (double-LBT) were fused to the 3′ end of *ompA* (encoding the outer membrane protein A) and placed under the control of the arabinose- inducible promoter ($P_{BAD}$) using the pBAD-*omp*A-*pbr*R vector[28] as a template (see Supporting Information (SI) for details). The resulting *lpp-ompA*-LBT expression plasmids were transformed into the indicated *E. coli* strains (SI Table S1).

**Expression of lpp-ompA-dLBT Constructs.** *E. coli* strains harboring *lpp-ompA*-dLBT expression plasmids were grown in LB media supplemented with 50 μg/mL ampicillin. Expression of *lpp-ompA*-dLBT was induced at mid-exponential phase using 0.002% arabinose for 3 h at 37 °C. The *E. coli* cells were harvested, washed once in 10 mM MES (2-(*N*-morpholino)- ethanesulfonic acid) pH 6.0, normalized by $OD_{600}$ and used in biosorption or luminescence experiments. Control cells contained the *lpp-ompA*-dLBTx8 expression plasmid but were not treated with arabinose. For *C. crescentus*, strains DMP146 (expressing 4 copies of LBT per RsaA protein) and JS4022 (control) were grown overnight at 30 °C in PYE supplemented

with 2 mM $CaCl_2$ as described previously[17] and washed as described for *E. coli*.

**Tb Adsorption Capacity Determination.** Washed *E. coli* and *C. crescentus* cells were incubated at an $OD_{600}$ of 0.25 in a solution containing 10 mM MES pH 6.0, 10 mM NaCl, and varying $Tb^{3+}$ concentrations (0−400 μM) for 30 min at RT prior to centrifugation at 20 000*g* for 8 min. The extracted supernatant was analyzed using inductively coupled plasma mass spectrometry (ICP-MS) to quantify $Tb^{3+}$ concentrations. Total adsorbed $Tb^{3+}$ was calculated by subtracting the $Tb^{3+}$ concentration remaining in the supernatant from the concentration of $Tb^{3+}$ in the control without bacterial cells. For dry cell weight determination, 6 mL of cells from reactions lacking $Tb^{3+}$ were dried overnight at 65 °C. Adsorption capacity was normalized to dry cell weight.

**Acid Leaching of REE-Containing Source Material.** Bull Hill borehole samples (43.5 m below land surface) were obtained from Rare Element Resources (Sundance, WY). Samples from the Round Top Mountain mineral deposit (El Paso, TX)[33] were crushed into fine particles using a mortar and pestle. Mine Tailings from Lower Radical and Togo Mines (near Montezuma, CO) were obtained as powder (<100 mesh:
< 150 μm) from USGS.[34] All samples were leached using aqua regia then adjusted to pH 6 (see SI for details). Following pH adjustment, the solubility of REEs in Bull Hill and Lower Radical leachates was unchanged, while the REE content of Togo leachates was reduced by 70% (data not shown).

**Biosorption Experiments with a Leachate from a Bull Hill Sediment Core.** Washed LBT-displayed and control *C. crescentus* CB2A and *E. coli* MG1655 cells were normalized to an $OD_{600}$ of 0.5. Adsorption experiments were performed under conditions where the total metal content was in excess of available surface sites. After a 30 min incubation with leachate (pH 6) at RT in 1.5 mL total volume, the supernatant was collected following centrifugation at 20 000*g* for 8 min and the metals remaining in solution were quantified by ICP-MS. Total adsorbed metals were calculated by subtracting the metal concentration remaining in the supernatant from the
concentration in the pH-adjusted (6.0) leachate. For desorption, the cells were washed once with an equal volume of 10 mM MES pH 6 then eluted with 1.5 mL of 5 mM citrate pH 6. The same adsorption/desorption procedure was used for no cell control experiments, but with a 10 mM MES pH 6 solution used in place of the cell suspension. The metal concentrations


DOI: 10.1021/acs.est.7b02414
*Environ. Sci. Technol.* 2017, 51, 13471−13480

in the no cell control were subtracted from the concentrations eluted from cells to account for abiotic precipitation during the experiment. This correction adjusted the final metal concentrations by less than 5%, with the exception of aluminum, where final concentrations were indistinguishable between biotic and abiotic conditions.

Biosorption Experiments with Round Top Mountain and Mine Tailing Leachates. Biosorption was performed under conditions where total metal content was in excess of available surface sites. LBT-displayed and control *E. coli* W3110 and WD101 cells were used at an $OD_{600}$ of 0.05 (~$1 \times 10^8$ cells/ml) in 5 mL total volume. After 1 h incubation with Round Top Mountain leachate (pH 6), the supernatant was collected following centrifugation at 20 000*g* for 8 min and the metals remaining in solution were quantified by ICP-MS as described above. For Lower Radical and Togo mine tailing leachates (pH 6), cells were immobilized on 0.2 μm cellulose acetate filters following the 1 h incubation as *E. coli* cells did not pellet well in these leachates.

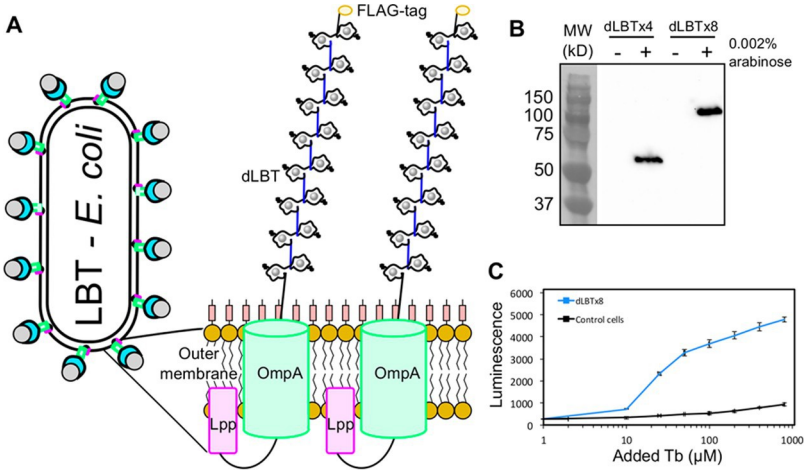


Figure 1. Surface display of dLBTs by *E. coli* for REE adsorption. (A) Schematic depicting the Lpp-OmpA mediated display of dLBTx8. REE-bound dLBTs (8 per OmpA molecule; black lines) are connected via the Muc1B spacer (blue lines) as described previously.[17] A Flag tag on the C-terminus was included for Western blot analysis. (B) Western blot of *lpp-ompA*-dLBTx4 and *lpp-ompA*-dLBTx8 expression after 3 h with (+) or without (−) 0.002% arabinose addition. (C) Luminescence (ex/em 280/544) signal of *E. coli* W3110 cells harboring pBAD-*lpp-ompA*-dLBTx8 (strain DMP489) with (dLBTx8) or without (control cells) arabinose induction as a function of $Tb^{3+}$ concentration. Error bars represent the standard deviation of biological triplicates.

ICP-MS. Ultrapure concentrated nitric acid was used to acidify (1% v/v) the samples and the commercial standard stock solutions prior to inductively coupled plasma mass spectrometry (ICP-MS) analysis. The instrument (Agilent 7900 with Ultra High Matrix Introduction) was standardized and operated at the University of Idaho in accordance with manufacturer's instructions.

Quantifying Biosorbent Efficacy. Several complementary metrics were used to quantify the efficacy of REE biosorption in control and bioengineered cells, with respect to both overall recovery and separation of non-REE metals. Fraction adsorbed was calculated by subtracting the metal concentration remaining in solution after biosorption from the initial concentration in the leachate then dividing by the initial leachate concentration. To assess the overall efficacy of REE separation by our adsorption and desorption process, we calculate a concentration factor (CF), defined as the ratio of the molar fraction of a particular metal relative to the total metal content present in the concentrate vs the initial leachate.

making an implicit assumption of constant $K_d$ behavior in a given solution, which is typically only valid within a narrow range of concentrations. In some cases, however, the concentration of certain non-REEs is less than or equal to some or all of the REEs, allowing the surface selectivity toward REEs to be more confidently constrained.

Following pH adjustment, the ore leachates evaluated in this study have high and variable aqueous metal concentrations. These metals can compete with REEs for both native and LBT surface sites, so it is necessary to determine the surface selectivity for the REEs relative to individual competing metals. We determined conditional selectivity coefficients ($K_s^{i,M}$),

$$K_s^{i,M} = \frac{K_d^i}{K_d^M} \quad (2)$$

Surface affinities of individual metals were compared by calculating distribution coefficients ($K_d$) with a given leachate and biosorbent:

$$K^i = \frac{n_i}{}$$

which quantifies the relative affinity of the surface for REE *i* relative to metal *M*. All selectivity coefficients were calculated relative to Nd, an REE of intermediate mass.

## RESULTS AND DISCUSSION



DOI: 10.1021/acs.est.7b02414
*Environ. Sci. Technol.* 2017, 51, 13471−13480

LBT Display Improves REE Adsorption Capacity in *E. coli*. To display LBT on the cell surface of *E. coli*, we utilized the outer membrane protein A (OmpA) fusion method[31]

spaced $c_i$ space(1)

space(Figure 1A). Up to eight copies of dLBT (16 single LBTs) were fused in tandem to the C-terminus of OmpA and the spacewhere $n_i$ is the net adsorbed concentration of a given element $i$ determined by calculating the change in aqueous fluid concentration and normalizing to cell surface area (6 $\mu m^2$/ cell[35]) per sample volume, and $c_i$ is the aqueous concentration of that element at equilibrium. For elements where the reaction with the leachate leads to desorption (e.g., Mg), the calculated value of $n$ is less than 0. For elements initially absent from the microbial suspension, we can make the assumption that $n$ is equivalent to the surface excess concentration. For surfaces with a finite number of surface sites, this parameter decreases monotonically with increasing surface excess because at higher adsorbed ion concentrations, fewer sites are available for continued adsorption (i.e., Langmuir adsorption). In the comparison of $K_d$ values among the competing metals, we are spaceexpression of the resulting OmpA-dLBT fusions was verified by Western blot (Figure 1B). Following induction with exogenous arabinose, OmpA-dLBT expression was observed for all dLBT variants with protein mobility inversely proportional to LBT copy number. Notably, both the dLBTx4 and dLBTx8 fusion proteins ran higher than their expected molecular weights. This anomalous migration is unsurprising for a membrane fusion protein and may reflect altered SDS binding to the dLBT-Muc1B repeats.[36] To confirm that the OmpA-LBTx8 fusion was functional for Tb adsorption, luminescence was quantified over a range of Tb concentrations, taking advantage of the tryptophan residue within LBT that sensitizes Tb-lumines- cence.[37] As expected, the arabinose-induced dLBTx8 strain exhibited increased luminescence compared to the uninduced space

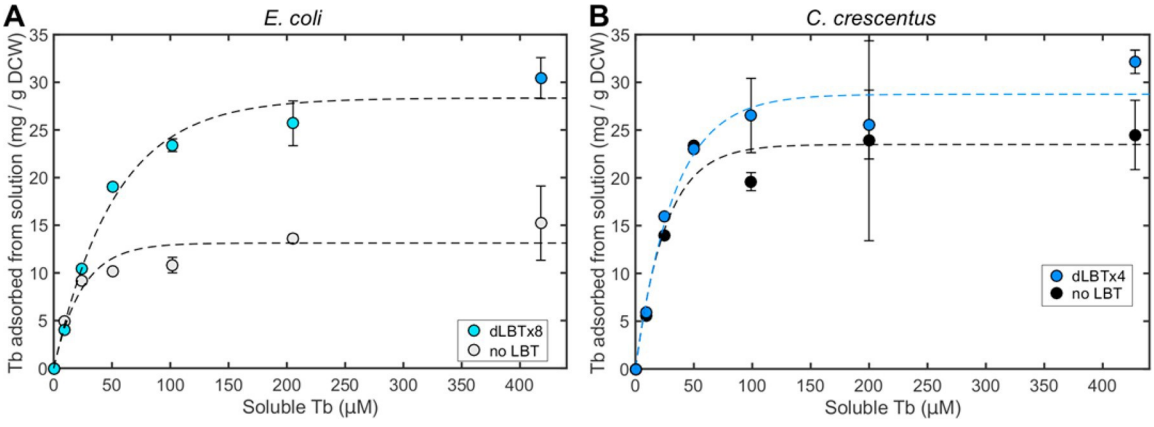


Figure 2. $Tb^{3+}$ adsorption capacity determination for *E. coli* and *C. crescentus* LBT-displayed cells. (A) $Tb^{3+}$ titration of *E. coli* W3110 cells harboring pBAD-*lpp-ompA*-dLBTx8 with (dLBTx8) or without (control cells) arabinose induction (B) $Tb^{3+}$ titration of *C. crescentus* displaying dLBTx4 via the S-layer (DMP146) and control cells with S-layer lacking LBTs (JS4022). Adsorbed metal was calculated by subtracting the metal concentration remaining in solution after adsorption from the initial added $Tb^{3+}$ concentration and then normalized to the dry cell weight (dcw). Adsorption capacity was determined by fitting the $Tb^{3+}$ adsorption data using the fit nonlinear regression model (fitnlm) in Matlab. Error bars represent the standard deviation of biological triplicates.

space

control (Figure 1C), suggesting that the OmpA-LBTx8 fusion is functional for REE binding.

To determine whether LBT expression enhanced the overall REE adsorption capacity of *E. coli*, adsorption isotherms were generated in a simplified buffered solution using Tb, a REE of high criticality.[38] *E. coli* expressing OmpA-dLBTx8 exhibited a 2-fold increase in $Tb^{3+}$ adsorption capacity compared to the uninduced control (28.3 ± 1.2 mg Tb/g dry cell weight (dcw) vs 13.1 ± 1.6 mg Tb/g dcw; Figure 2A). In contrast to *E. coli*, LBT display via the S-layer in *C. crescentus*[17] only marginally increased the adsorption capacity (28.7 ± 2.1 mg Tb/g dcw vs 23.5 ± 2.2 mg Tb/g dcw for LBT and control strains, respectively; Figure 2B). The greater effect of LBT in the *E. coli* system was consistent with the theoretical estimate of a 5-fold increase in the number of LBT molecules per cell; there are ∼100,000 molecules of OmpA per *E. coli*[32] compared to ∼40 000 RsaA molecules per *C. crescentus*[39] and the LBT copy number was 16 per OmpA and 8 per S-layer. However, it is worth noting that insertion of Lpp-OmpA-dLBTx8 into the outer membrane may have indirectly altered the cell surface functional groups. Since many factors likely contribute to REE adsorption on the bacterial cell surface, it is conceivable that the increased adsorption capacity of LBT-displayed *E. coli* may not have been mediated exclusively by LBT expression.

Previous studies using the OmpA display system to express ligands on the cell surface for metal adsorption (e.g., Cd, Au or Pb) have reported a greater (9−12-fold) increase in metal adsorption capacity compared to native strains.[28,40,41] However, the overall adsorption capacity for these target metals was lower (1−10 mg/g dcw for induced cells[28,40,41]) than that achieved for REEs. The high REE adsorption by control *E. coli* and *C. crescentus* cells indicates a significant role of native cell surface functional groups in REE binding. Additionally, given the difference in adsorption capacity between control *E. coli* and *C. crescentus* cells (13.1 compared to 23.5 mg Tb/g dcw, respectively), strategic selection of the adsorbent organism is one potential means to improve REE adsorption


DOI: 10.1021/acs.est.7b02414
*Environ. Sci. Technol.* 2017, 51, 13471−13480

capacity. Nevertheless, the 28 mg/g DCW capacity of LBT-displayed *E. coli* and *C. crescentus* cells is comparable to other reported adsorbents, including salmon milt (50.1 mg/g[42]), activated

spacecarbon (∼0.1−145 mg/g[43,44]), ligand grafted silica (167 mg/ g[45]) and cation exchange resin (∼20−120 mg/g[46]).

Biosorption Performance with High-Grade REE Feed- stocks. To test the efficacy of *E. coli* and *C. crescentus* LBT-display systems for REE extraction from an industrially relevant REE source, we performed biosorption assays with the acid leachates of sediment core samples collected from the Bull Hill Mine (WY). Biosorption assays were performed at pH 6.0 as a previous study revealed optimal REE adsorption by LBT- displayed *Caulobacter* at this pH.[17] Characterization of the metal concentrations of the pH (6.0)-adjusted leachate revealed that REEs (e.g., La, Ce, Nd, Pr, and Y) remained soluble after pH adjustment (data not shown) and comprised ∼30% by mass of the total metal content (Figure 3). The predominant non- REEs included Mn, Ba, Zn, and Sr, with Mn comprising 50% by mass of the total metal content (Figure 3C).

LBT-displayed *E. coli* and *C. crescentus* exhibited similar REE adsorption efficacy; greater than 86% of the Ce, Pr, Nd, and Y content was adsorbed by LBT-displayed *E. coli* compared to 92% for LBT-displayed *C. crescentus* (Figure 3A,B; SI Table S2). Minimal adsorption (<10%) was observed for the predominant non-REE cations present in the leachate, indicating selective REE adsorption by both cell types. Consistent with the adsorption capacity experiments (Figure 2), the biggest difference observed between the two bacterial species was the REEs adsorption by control strains lacking LBT; *C. crescentus* adsorbed 59% of REEs compared to only 24% by *E. coli* (Figure 3A,B; SI Table S2). Thus, although the adsorption capacity of both species benefit from LBT display, LBT display in *E. coli* yielded a greater improvement in REE adsorption capacity.

To recover adsorbed REEs from the cell surface, desorption was performed using citrate (5 mM, pH 6), an eluent previously shown to effectively recover $Tb^{3+}$ from *C. crescentus*.[17] Treatment of metal-loaded cells with a volume of citrate equivalent to that of the leachate eluted the vast majority of REEs from the surface of cells (Figure 3A,B). Following desorption, the eluent metal content was greater than 90% by mass REEs for both LBT and non-LBT cells (Table 1; Figure 3C), with concentration factors for REEs ranging from 3.4 to
4.3 for LBT-displayed *C. crescentus* and 1.8 to 3.6 for LBT- displayed *E. coli* (SI Table S2). Collectively, these results
space

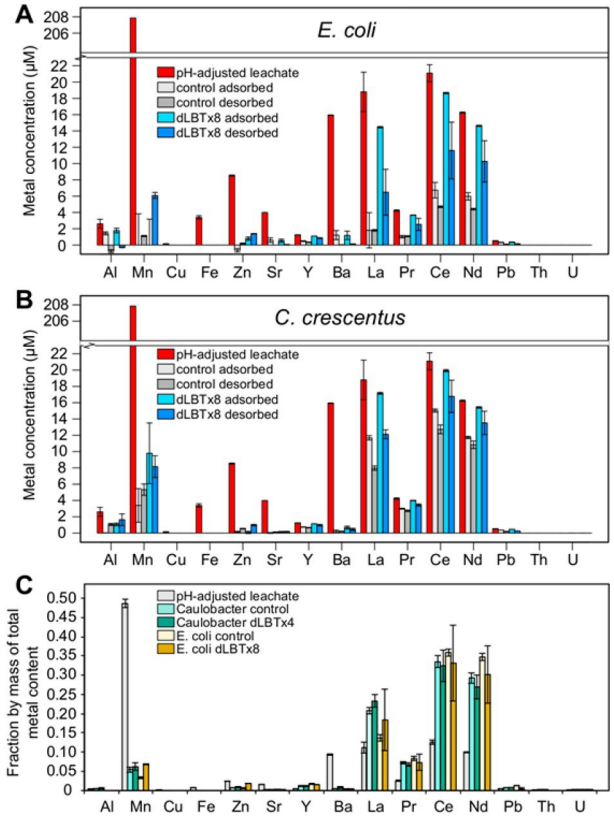


Figure 3. Metal adsorption profile of leachates of Bull Hill sediment core samples. (A) The metal concentration profile following adsorption with LBT-displayed (*lpp-omp*A-dLBTx8, induced with arabinose) and control (*lpp-omp*A-dLBTx8, no arabinose induction) *E. coli* MG1655 cells (DMP281) and desorption from the cell surface
using an equal volume of 5 mM citrate (see methods). (B) The metal concentration profile following adsorption with LBT-displayed (DMP146) and control (JS4022) *C. crescentus* cells and desorption from the cell surface using 5 mM citrate (see Materials and Methods). The metal concentration profile of the pH-adjusted (6.0) leachate is depicted in A and B for comparison. (C) Displays the fraction by mass for metal M of the total metal content present in the pH-adjusted (6.0) leachate before adsorption and after an adsorption/desorption cycle with LBT-displayed and control *E. coli* and *C. crescentus* cells.

Table 1. REE Purity in Leachates from Bull Hill Samples

spaceSelective Adsorption of REEs from Leachates with Low REE Content. To further evaluate the efficacy of *E. coli* LBT-displayed strains for REE extraction from practical feedstocks, biosorption assays were performed with leachates of


DOI: 10.1021/acs.est.7b02414
*Environ. Sci. Technol.* 2017, 51, 13471−13480

a Round Top Mountain mineral deposit (El Paso, TX)[33] and tailings from two Colorado mines (Lower Radical and Togo Mines, near Montezuma, CO).[34] Following acid leaching and pH-adjustment (pH 6.0), REEs comprised 0.9%, 5.5%, and 0.5% by mass of the total metals for the Lower Radical, Round Top Mountain, and Togo leachates, respectively. Each leachate contained the same 11 REEs present at nM concentrations (except Y was at 3 μM in Round Top) and several non-REE metals, most of which were present at concentrations orders of magnitude higher than the REEs (Figure 4A; SI Table S3). Given the prevalence of competitively sorbing metals, these leachates provided an excellent test for REE adsorption selectivity.

To evaluate the relative affinity of cell surfaces for individual metals, we calculated a distribution coefficient ($K_d$) for each metal between the cell surface and aqueous solution (SI Table S4). Both control and LBT-displayed strains adsorbed REEs with high affinity relative to most non-REEs (Figure 4B−D; SI Table S4). Importantly, functionalizing the cell surface with LBTs enhanced the $K_d$ values for each REE by 2 to 10-fold across all leachates (Figure 4E; see below for discussion of individual REEs) with total REE adsorption ranging from 42 to 92% compared to 19 to 70% for control cells (SI Figure S1). Little to no adsorption was observed for Ca, Ba, Zn, Mg, Na, K, Mn, and Rb by either strain despite their high abundance in the leachates (<10% adsorbed, $K_d$ < 0.5; Figure 4B−D; SI Figure S1). The concentration of Mg in solution actually increased following adsorption (SI Table S3), suggestive of net desorption from the cell surface through ion exchange with metals in the leachate that have higher cell surface affinity. The highest $K_d$ values among non-REEs metals were for Al, Cu, Ga, and Pb ($K_d$ > 1; Figure 4B−D; SI Table S4). However, in contrast to REEs, there was a minimal difference (<2-fold) in the $K_d$ values for these metals between LBT-displayed and control strains, with the exception of Cu where LBT display enhanced the $K_d$ by 3−3.6-fold (Figure 4E).

To compare the surface selectivity for REEs relative to non- REEs, conditional selectivity coefficients were calculated for Nd achates (Table 2; SI Table S5). The $K^{Nd,M}$ represents the surface comparisons among leachates with varied metal content. We note

s]
s]

ease

s

| sample | percent REE by mass of total metal content[a] |
|---|---|
| Bull Hill leachate pH 6 | 37 (0.02) |
| Eluent from *C. crescentus* control | 91 (0.05) |
| Eluent from *C. crescentus* dLBTx8 | 91 (0.15) |
| Eluent from *E. coli* control | 94 (0.20) |
| Eluent from *E. coli* dLBTx8 | 90 (0.15) |

[a]Values in the parentheses represent one standard deviation.

showed that both LBT and non-LBT strains selectively enriched for REEs through surface adsorption, and that LBT display increased adsorption capacity without sacrificing selectivity. However, the high overall recovery and separation efficiency may not necessarily be representative of lower-grade REE feedstocks. Given the greater REE adsorption enhance- ment of surface-displayed LBT in *E. coli* compared to *C. crescentus*, we chose *E. coli* for further characterization of more complex leachates.

spacewith increasing concentration under otherwise fixed solution conditions. Thus, given the fixed composition of these feedstocks, it is not possible to obtain thermodynamic selectivity coefficients for non-REEs relative to REEs, or to quantitatively compare $K_d$ values. Nevertheless, comparisons of $K^{Nd,M}$ values for REEs and non-REEs of similar concentration (e.g., Pb, Cu, Ga, Ba, Cd concentrations are less than or equal to some or all REE concentrations) and between LBT and non-LBT strains are expected to capture or underestimate surface selectivity toward the REEs.

Consistent with prior reports on preferential adsorption of REEs over non-REEs in several bacterial species,[22,23] the *E. coli* control strain exhibited preferential adsorption of Nd over all non-REEs except for Ga and Al, which had $K_s^{Nd,M}$ values close to 1 (∼0.8 to 1.3 for Al and ∼0.3 to 1.7 for Ga; Table 2). The

space


DOI: 10.1021/acs.est.7b02414
*Environ. Sci. Technol.* 2017, 51, 13471−13480

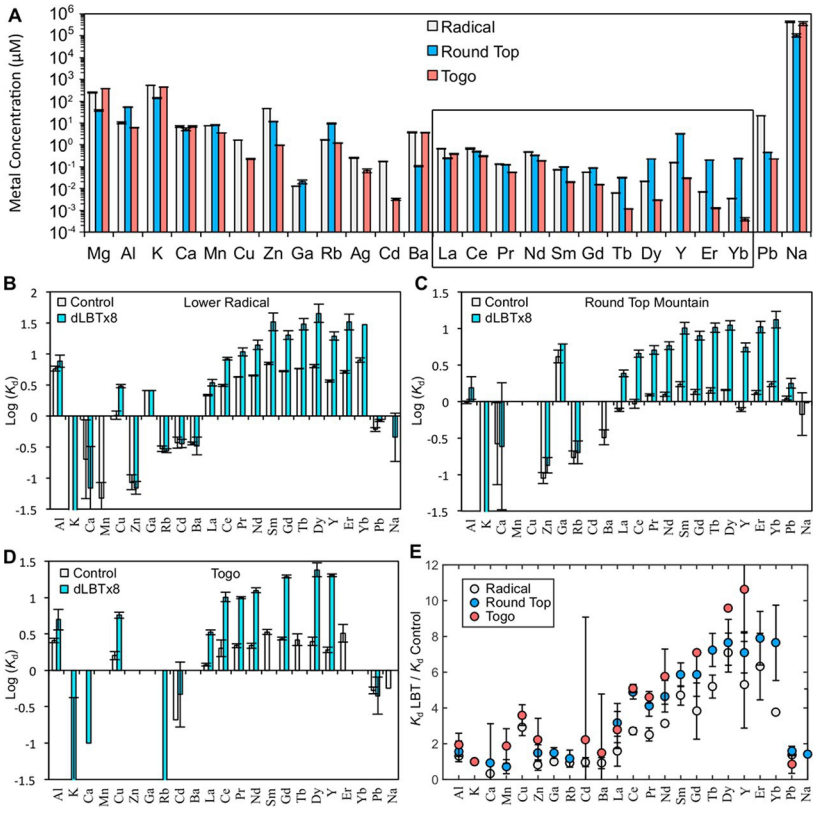


Figure 4. Selective adsorption of REEs from Lower Radical, Togo, and Round Top Mountain leachates. (A) Metal concentration profile of pH- adjusted (6.0) leachates prior to adsorption. The 11 REEs present are boxed. Note that the high Na levels were a result of NaOH added during pH adjustment. Metal distribution coefficient ($K_d$) for LBT-displayed (*lpp-ompA*-dLBTx8, induced with arabinose) and control (*lpp-ompA*-dLBTx8, no arabinose induction) *E. coli* W3110 cells (DMP489) for Lower Radical (B), Round Top Mountain (C), and Togo leachates (D). For Togo leachates, the concentrations of Tb, Er and Yb remaining in solution after biosorption with the LBT-displayed strain were below the detection limit of ICP-MS, and thus, $K_d$ values could not be accurately determined. See SI Figure S1 for plots of the fraction of each metal bound by both strains. (E) Ratio of metal distribution coefficients for the LBT-displayed strain relative to the control. Ratios greater than 1 reflected more efficient extraction by the LBT strain. For all plots, REEs are listed in order of decreasing atomic radii,[54] and error bars represent the standard deviation of biological triplicates. Note that although we quantified Na concentrations, these were not factored into the total metal concentrations as the majority of Na was added exogenously during pH-adjustment.

Table 2. Conditional Selectivity Coefficients ($K^{Nd,M}$) for Nd[a]

| strain[b] | leachate | Al | Cu | Zn | Ga | Cd | Pb | Dy |
|---|---|---|---|---|---|---|---|---|
| control cells | RAD[c] | 0.77 (0.06) | 4.35 (0.66) | 52.28 (14.45) | 1.74 (0.02) | 12.07 (2.48) | 7.4 (0.54) | 0.7 (0.04) |
| dLBTx8 | RAD | 1.83 (0.52) | 4.62 (0.85) | 202.58 (59.23) | 5.44 (0.93) | 38.87 (9.04) | 16.57 (2.94) | 0.31 (0.11) |
| control cells | RTM[d] | 1.29 (0.09) | ND | 14.06 (2.53) | 0.3 (0.06) | ND | 1.12 (0.1) | 0.87 (0.06) |
| dLBTx8 | RTM | 3.81 (1.47) | ND | 43.65 (11.88) | 0.95 (0.12) | ND | 3.29 (0.64) | 0.52 (0.1) |
| control cells | TG[e] | 0.84 (0.09) | 1.36 (0.2) | ND | ND | 10.34 (30.35) | 4.13 (0.56) | 0.87 (0.13) |
| dLBTx8 | TG | 2.52 (0.84) | 2.18 (0.26) | ND | ND | 26.93 (27.81) | 28.03 (16.48) | 0.52 (0.12) |

[a]See SI Table S5 for full list of $K^{Nd,M}$ values. [b]*E. coli* W3110 cells harboring pBAD-*lpp-ompA*-dLBTx8 with (dLBTx8) or without (control cells) arabinose induction.

[c]RAD: Lower Radical.

[d]RTM: Round Top Mountain.

[e]TG: Togo.

lack of surface selectivity for Nd compared with Ga and Al is likely due to the fact that these are the only non-REE metals in the leachates that predominately exist in a + 3 oxidation state. Al was found to be a more effective competitor for REE binding to the *Pseudomonas aeruginosa* cell surface compared to tested [20] indicate that the REEs effectively compete with non-REEs for adsorption to the native cell surface.

For LBT-displayed cells, $K_s^{Nd,M}$ values >1 were observed for all non-REE metals, indicative of preferential adsorption of Nd over non-REE elements (Table 2; SI Table S5). Furthermore, comparison of the $K^{Nd,M}$ values for LBT-displayed cells relative to *B. subtilis* with high affinities relative to all divalent cations, except for uranyl that is known to form strong specific complexes with carboxylate ligands.[21] Lastly, there was a slight preference of the *E. coli* surface for Nd over Cu given the $K_s^{Nd,Cu}$ values of 1.4 and 4.4 for Togo and Lower Radical leachates, respectively (Table 2). Collectively, these data


DOI: 10.1021/acs.est.7b02414
*Environ. Sci. Technol.* 2017, 51, 13471−13480

spaceto the control revealed an enhancement in Nd selectivity for all metals except Cu, where the $K_s^{Nd,Cu}$ values were similar for both cell types (Figure 5A; Table 2). Thus, Cu is the only element that competed as effectively as REEs for the LBT-displayed *E. coli* surface, suggesting competitive binding of Cu to LBT. Consistently, Cu was found to be an effective non-REE competitor for both purified LBT[47] and LBT-displayed on the space

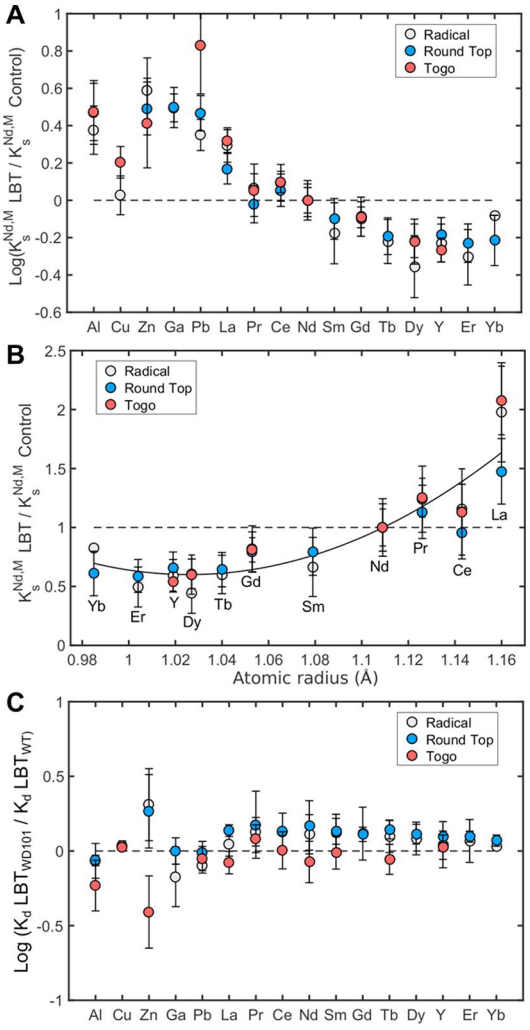


Figure 5. Impact of LBTs on metal competition for the *E. coli* cell surface. (A) Comparison of REE binding selectivity for LBT-displayed (*lpp-ompA*-dLBTx8, induced with arabinose) and control (*lpp-ompA*- dLBTx8, no arabinose induction) cells for Lower Radical, Round Top Mountain, and Togo leachates. Conditional selectivity coefficients ($K_s^{Nd,M}$) for Nd were determined to quantify the affinity of Nd for the cell surface relative to REEs and select non-REEs (M). Data are depicted as the log transformed ratio of the $K_s^{Nd,M}$ in LBT-displayed cells relative to control cells. Values greater than 0 reflected an enhanced selectivity for Nd relative to a specific metal by LBT- displayed cells in comparison to control cells. See SI Table S5 for a complete list of $K_s^{Nd,M}$ values. Error bars represent the relative error of biological triplicates. (B) Depicts the dependence of $K_s^{Nd,M}$ ratios for LBT-displayed cells relative to control cells on the atomic radii of REE elements.[54] Values greater than 1 reflected an enhanced selectivity for Nd relative to the specific REE by LBT-displayed cells in comparison to control cells. The black line is added to depict the trend ($R^2$ = 0.82). Error bars represent the standard deviation of biological triplicates.
(C) Comparison of metal distribution coefficients ($K_d$) for the LBT-displayed WD101 strain (DMP488) relative to the LBT-displayed wild type (W3110; DMP489). The ratio of $K_d$ values is plotted for REEs and select non-REEs. Error bars represent the relative error of biological triplicates.

surface of *C. crescentus*,[17] and is known to form the most stable complexes of first-row divalent metal cations.[48] Thus, for REE source materials with high Cu content, adding a preprocessing step to reduce Cu levels would likely be advantageous. In contrast to Cu, the larger $K_s^{Nd,M}$ values for LBT-displayed cells

spacerelative to control cells for Al, Ga and Pb suggested that these metals are poorer competitors for the LBT-displayed *E. coli* surface (Figure 5A; Table 2). Collectively, these data indicated that functionalizing the cell surface with LBTs significantly enhances the cell surface selectivity for REEs.

LBT Display Enhances Selectivity for Heavy HREEs. The adsorption preference of *E. coli* cells for REEs was not uniform. In particular, the distribution coefficients correlated with the atomic radii of the REEs; REEs with larger radii (e.g., La, Pr, Ce) were depleted on the cell surfaces, while those with smaller radii (Tb, Dy, Er, Yb) were enriched (Figure 4B−E). As REEs with small radii are traditionally categorized as heavy REEs (HREEs), this result was largely consistent with previous


DOI: 10.1021/acs.est.7b02414
*Environ. Sci. Technol.* 2017, 51, 13471−13480

reports of preferential adsorption of HREEs over light REEs (LREEs) by both Gram-positive and Gram-negative bacteria.[16,24,25] To determine whether the HREE enrichment was enhanced in the LBT-displayed strain, the ratio of selectivity coefficients of LBT vs control strains was plotted as a function of atomic radii of REEs. The selectivity enhancement mediated by LBT display increased systematically with decreasing atomic radius for La through Dy (Figure 5B). A further enhancement in selectivity was not observed for REEs smaller than Dy. This trend was reminiscent of the binding free energy measurements of LBTs for REEs, which exhibit a similar dependence on atomic radii with a free energy minimum occurring for Tb.[37]

These results highlight two features of LBT-displayed strains that have important implications for application in REE extraction. First, although the cell surface in general prefers to adsorb REEs over non-REEs, functionalization with LBT further enhances this preference, increasing the separating power of REE vs non-REEs, including those that are tight cell surface binders (e.g., Al and Pb). Second, the enhanced selectivity for REEs with smaller radii highlights a promising path for the use of LBT-displayed cells for preferential enrichment of HREEs. REEs are notoriously difficult to separate from each other due to their similar physicochemical properties with dozens of solvent extraction steps required for purification of individual REEs.[9] Similar to the recently reported pH-dependent-REE desorption scheme that achieved impressive enrichment for some HREEs,[26] improved separation among REEs is expected in the LBT-displayed strains and is part of our ongoing effort.

Lipid A Phosphate Groups of LPS Have Minimal Effect on REE and Non-REE Biosorption. Based on results from previous sections, it is clear that native cell surface functional groups make a significant contribution to REE and non-REE metal adsorption. Given the enhanced selectivity for REEs observed with LBT-functionalized cells, we hypothesized that decreasing the number of native functional groups on the cell surface may further improve the REE binding selectivity. Numerous studies have implicated cell surface carboxylate and phosphate sites as the predominate mediators of metal adsorption.[15] As an initial step, we employed a well- characterized *E. coli* mutant strain (WD101) that produces lipopolysaccharides (LPS) with functionalized phosphate groups.[49] Strain WD101 carries a mutation that results in constitutive modification of lipid A phosphate groups with L-4- aminoarabinose (L-Ara4N) and phosphoethanolamine, thereby reducing the number of free phosphate sites on the cell surface.[50] A similar modification in *Salmonella enterica* significantly reduced Fe adsorption relative to the wild type control.[51]

space

To evaluate the performance of LBT-displayed WD101, biosorption was conducted with the Round Top, Togo and Radical leachates. The distribution coefficients for WD101 were nearly identical to the isogenic *E. coli* strain (WT), indicative of similar extraction efficiencies for both REEs and non-REEs, including Al, Ga, Pb, and Cu (Figure 5C; SI Table S4). Therefore, the contribution of lipid A phosphates to metal adsorption appeared relatively small under the conditions tested. The results are largely consistent with studies that indicate a greater role for carboxylate functional groups in metal/REE adsorption at pH values around 6. Fein et al. found a strong correlation between fitted metal-carboxyl bacterial surface stability constants and metal-acetate aqueous stability constants for both divalent (e.g., $Pb^{2+}$, $UO^{2+}$) and trivalent ($Nd^{3+}$, $Al^{3+}$) ions, suggesting that cell surface carboxylates have a significant role in metal adsorption.[21] In addition, EXAFS data revealed that the contribution of carboxylates increased with increasing pH up to 6 (values higher than 6 were not tested),[52] while contributions from phosphate groups appeared to predominate at low pH,[24,53] conditions under which LBT- REE binding is greatly diminished.[17]

This study was undertaken to test the efficacy of a biosorption approach for REE recovery and refinement from complex feedstocks. Our data indicate that functionalizing a bacterial cell surface with LBTs enhances both adsorption capacity and selectivity, enabling the separation of REEs from the vast majority of non-REE impurities with a single adsorption step. Given the promising results with mine tailings leachates, biosorption may also be amenable to other low-grade REE feedstocks, including coal byproducts, ion adsorption$^{2}$clays, and geothermal brines. However, feedstocks with matrix compositions (e.g., high phosphate content) that limit REE solubility at pH 6 are unlikely to be compatible with this bioadsorption platform. Furthermore, in order to process large volumes of low-grade materials, significant process engineering and scaling efforts will be required. Development of a cell immobilization system would facilitate a continuous flow operation to achieve REE separation without the need for filtration or centrifugation. Various cell immobilization techniques are currently under investigation, including biofilm formation on abiotic surfaces and cell encapsulation within hydrogels. Ultimately, development of an industrial-scale REE extraction process will require integration of biosorption into a broader extraction scheme that includes solubilization of solid feedstocks through leaching, pH-adjustment prior to bio- sorption, and post-biosorption steps such as oxalic acid precipitation and roasting to produce total rare earth oxides.

## ASSOCIATED CONTENT

### Supporting Information

The Supporting Information is available free of charge on the ACS Publications website at DOI: 10.1021/acs.est.7b02414.

Figure S1, Metal adsorption profiles for Lower Radical, Round Top Mountain and Togo leachates (PDF) Table S1, strains and plasmids used; Table S2, Bull Hill adsorption and desorption data; Table S3, metals adsorbed by control and LBT-displayed cells; Table S4, distribution metal coefficients ($K_d$); Table S5, condi- tional selectivity coefficients ($K^{Nd,M}$) (XLSX)

s



DOI: 10.1021/acs.est.7b02414
*Environ. Sci. Technol.* 2017, 51, 13471−13480

## spaceAUTHOR INFORMATION

Corresponding Author

*E-mail: jiao1@llnl.gov.

ORCID

Yongqin Jiao: 0000-0002-6798-5823

Notes

The authors declare the following competing financial interest(s): Lawrence Livermore National Laboratory has filed a patent application related to the technology described in this work to the United States Patent and Trademark Office.

## ACKNOWLEDGMENTS

We are grateful for the ICP-MS analysis provided by Debbie Lacroix at University of Idaho. We thank Adrian Van Rythoven at Rare Earth Resources for providing Bull Hill sediment cores, Phil Goodell and Lixin Jin at the University of Texas at El Paso for providing Round Top samples, Philip Hageman at the USGS for providing mine tailing samples and leaching advice, Jing Zhao at Peking University for providing the pBAD-lpp-ompA-pbrR plasmid, Michael Trent at University of Georgia for providing the *E. coli* W3110 and WD101 strains, and John Smit at University of British Columbia for providing the *Caulobacter* CB2A strain. This research is supported by the Critical Materials Institute, an Energy Innovation Hub funded by the U.S. Department of Energy, Office of Energy Efficiency and Renewable Energy, Advanced Manufacturing Office. AB was supported by the LLNL Livermore Graduate Scholar Program. This work was performed under the auspices of the U.S. Department of Energy by Lawrence Livermore National Laboratory under Contract DEAC52-07NA27344 (LLNL-JRNL-730719) and by Idaho National Laboratory under DOE Idaho Operations Office Contract DE-AC07- 05ID14517 (INL/JOU-17-41899). The authors declare no competing financial interest.

## REFERENCES

(1) Du, X.; Graedel, T. E. Global in-use stocks of the rare Earth elements: a first estimate. *Environ. Sci. Technol.* 2011, *45* (9), 4096−101.

(2) Stone, R. As China's Rare Earth R&D Becomes Ever More Rarefied, Others Tremble. *Science* 2009, *325* (5946), 1336−1337.

(3) Alonso, E.; Sherman, A. M.; Wallington, T. J.; Everson, M. P.; Field, F. R.; Roth, R.; Kirchain, R. E. Evaluating rare earth element availability: a case with revolutionary demand from clean technologies. *Environ. Sci. Technol.* 2012, *46* (6), 3406−14.

(4) Massari, S.; Ruberti, M. Rare earth elements as critical raw materials: Focus on international markets and future strategies. *Resour. Policy* 2013, *38* (1), 36−43.

(5) Zhang, W. C.; Rezaee, M.; Bhagavatula, A.; Li, Y. G.; Groppo, J.; Honaker, R. A Review of the Occurrence and Promising Recovery Methods of Rare Earth Elements from Coal and Coal By-Products. *Int. J. Coal Prep. Util.* 2015, *35* (6), 295−330.

(6) Rozelle, P. L.; Khadilkar, A. B.; Pulati, N.; Soundarrajan, N.; Klima, M. S.; Mosser, M. M.; Miller, C. E.; Pisupati, S. V. A Study on Removal of Rare Earth Elements from U.S. Coal Byproducts by Ion Exchange. *Metall Mater. Trans B* 2016, *3* (1), 6−17.

(7) Finster, M.; Clark, C.; Schroeder, J.; Martino, L. Geothermal produced fluids: Characteristics, treatment technologies, and manage- ment options. *Renewable Sustainable Energy Rev.* 2015, *50*, 952−966.

(8) Wood, S. A., Behavior Of Rare Earth Elements In Geothermal Systems: A New Exploration/Exploitation Tool? *Dept Of Energy, Geoth Reservoir Technol. Res, Dev And Demo* 2001.

(9) spaceXie, F.; Zhang, T. A.; Dreisinger, D.; Doyle, F. A critical review on solvent extraction of rare earths from aqueous solutions. *Miner. Eng.* 2014, *56*, 10−28.

(10) Priya, A.; Hait, S. Comparative assessment of metallurgical recovery of metals from electronic waste with special emphasis on bioleaching. *Environ. Sci. Pollut. Res.* 2017, *24* (8), 6989−7008.

(11) Jha, M. K.; Kumari, A.; Panda, R.; Rajesh Kumar, J.; Yoo, K.; Lee, J. Y. Review on hydrometallurgical recovery of rare earth metals. *Hydrometallurgy* 2016, *165* (Part 1), 2−26.

(12) Li, P. S.; Tao, H. C. Cell surface engineering of microorganisms towards adsorption of heavy metals. *Crit. Rev. Microbiol.* 2015, *41* (2), 140−9.

(13) Zhuang, W. Q.; Fitts, J. P.; Ajo-Franklin, C. M.; Maes, S.; Alvarez-Cohen, L.; Hennebel, T. Recovery of critical metals using biometallurgy. *Curr. Opin. Biotechnol.* 2015, *33*, 327−335.

(14) Mejare, M.; Bulow, L. Metal-binding proteins and peptides in bioremediation and phytoremediation of heavy metals. *Trends Biotechnol.* 2001, *19* (2), 67−73.

(15) Moriwaki, H.; Yamamoto, H. Interactions of microorganisms with rare earth ions and their utilization for separation and environmental technology. *Appl. Microbiol. Biotechnol.* 2013, *97* (1), 1−8.

(16) Takahashi, Y.; Chaĥellier, X.; Hattori, K. H.; Kato, K.; Fortin, D. Adsorption of rare earth elements onto bacterial cell walls and its implication for REE sorption onto natural microbial mats. *Chem. Geol.* 2005, *219* (1−4), 53−67.

(17) Park, D. M.; Reed, D. W.; Yung, M. C.; Eslamimanesh, A.;



DOI: 10.1021/acs.est.7b02414
*Environ. Sci. Technol.* 2017, 51, 13471−13480

Lencka, M. M.; Anderko, A.; Fujita, Y.; Riman, R. E.; Navrotsky, A.; Jiao, Y. Bioadsorption of Rare Earth Elements through Cell Surface Display of Lanthanide Binding Tags. *Environ. Sci. Technol.* 2016, *50* (5), 2735−42.
(18) Wu, Y.; Li, T.; Yang, L. Mechanisms of removing pollutants from aqueous solutions by microorganisms and their aggregates: A review. *Bioresour. Technol.* 2012, *107*, 10−18.
(19) Vannela, R.; Verma, S. K. Co2+, Cu2+, and Zn2+ accumulation by cyanobacterium *Spirulina platensis*. *Biotechnol. Prog.* 2006, *22* (5), 1282−93.
(20) Texier, A.-C.; Andres̀, Y.; Le Cloirec, P. Selective Biosorption of Lanthanide (La, Eu, Yb) Ions by *Pseudomonas aeruginosa*. *Environ. Sci. Technol.* 1999, *33* (3), 489−495.
(21) Fein, J. B.; Martin, A. M.; Wightman, P. G. Metal adsorption onto bacterial surfaces: development of a predictive approach. *Geochim. Cosmochim. Acta* 2001, *65* (23), 4267−4273.
(22) Tsuruta, T. Selective accumulation of light or heavy rare earth elements using gram-positive bacteria. *Colloids Surf., B* 2006, *52* (2), 117−122.
(23) Moriwaki, H.; Koide, R.; Yoshikawa, R.; Warabino, Y.; Yamamoto, H. Adsorption of rare earth ions onto the cell walls of wild-type and lipoteichoic acid-defective strains of *Bacillus subtilis*. *Appl. Microbiol. Biotechnol.* 2013, *97* (8), 3721−8.
(24) Ngwenya, B. T.; Mosselmans, J. F. W.; Magennis, M.; Atkinson, K. D.; Tourney, J.; Olive, V.; Ellam, R. M. Macroscopic and spectroscopic analysis of lanthanide adsorption to bacterial cells. *Geochim. Cosmochim. Acta* 2009, *73* (11), 3134−3147.
(25) Takahashi, Y.; Hirata, T.; Shimizu, H.; Ozaki, T.; Fortin, D. A rare earth element signature of bacteria in natural waters? *Chem. Geol.* 2007, *244* (3−4), 569−583.
(26) Bonificio, W. D.; Clarke, D. R. Rare-Earth Separation Using Bacteria. *Environ. Sci. Technol. Lett.* 2016, *3* (4), 180−184.
(27) Hennebel, T.; Boon, N.; Maes, S.; Lenz, M. Biotechnologies for critical raw material recovery from primary and secondary sources: R&D priorities and future perspectives. *New Biotechnol.* 2015, *32* (1), 121−7.
(28) Wei, W.; Liu, X.; Sun, P.; Wang, X.; Zhu, H.; Hong, M.; Mao, Z. W.; Zhao, J. Simple whole-cell biodetection and bioremediation of heavy metals based on an engineered lead-specific operon. *Environ. Sci. Technol.* 2014, *48* (6), 3363−71.
(29) spaceXu, Z.; Lei, Y.; Patel, J. Bioremediation of soluble heavy metals with recombinant *Caulobacter crescentus*. *Bioeng Bugs* 2010, *1* (3), 207−12.
(30) Allen, K. N.; Imperiali, B. Lanthanide-tagged proteins an illuminating partnership. *Curr. Opin. Chem. Biol.* 2010, *1̀* (2), 247− 254.
(31) Francisco, J. A.; Earhart, C. F.; Georgiou, G. Transport and anchoring of beta-lactamase to the external surface of *Escherichia coli*. *Proc. Natl. Acad. Sci. U. S. A.* 1992, *89* (7), 2713−7.
(32) Koebnik, R.; Locher, K. P.; Van Gelder, P. Structure and function of bacterial outer membrane proteins: barrels in a nutshell. *Mol. Microbiol.* 2000, *37* (2), 239−53.
(33) Pingitore, N.; Clague, J.; Gorski, D. Round Top Mountain rhyolite (Texas, USA), a massive, unique Y-bearing-fluorite-hosted heavy rare earth element (HREE) deposit. *J. Rare Earths* 2014, *32* (1), 90−96.
(34) Hageman, P. L. *Use of short-term (5-minute) and long-term (18-h) leaching tests to characterize, fingerprint, and rank mine-waste material from historical mines in the Deer Creek, Snake River, and Clear Creek Watersheds in and around the Montezuma Mining District, Colorado; 2004−5104*; U.S. Geological Survey, Scientific Investigations Report, 2004.
(35) Phillips, R.; Kondev, J.; Theriot, J. *Physical biology of the cell*. Garland Science: New York, 2009; p xxiv, 807 p.
(36) Rath, A.; Glibowicka, M.; Nadeau, V. G.; Chen, G.; Deber, C. M. Detergent binding explains anomalous SDS-PAGE migration of membrane proteins. *Proc. Natl. Acad. Sci. U. S. A.* 2009, *106* (6), 1760−5.
(37) Nitz, M.; Sherawat, M.; Franz, K. J.; Peisach, E.; Allen, K. N.; Imperiali, B. Structural origin of the high affinity of a chemically evolved lanthanide-binding peptide. *Angew. Chem., Int. Ed.* 2004, *43* (28), 3682−5.
(38) Bauer, D.; Diamond, D.; Li, J.; Sandalow, D.; Telleen, P.; Wanner, B. *U.S. Department of Energy Critical Materials Strategy*; None; TRN: US201104%%69 United States 10.2172/1000846 TRN: US201104%%69 DOEEE English; ; None: 2010; p Medium: ED.
(39) Nomellini, J. F.; Kupcu, S.; Sleytr, U. B.; Smit, J. Factors controlling in vitro recrystallization of the *Caulobacter crescentus* paracrystalline S-layer. *J. Bacteriol.* 1997, *179* (20), 6349−54.
(40) Wei, W.; Zhu, T.; Wang, Y.; Yang, H.; Hao, Z.; Chen, P. R.; Zhao, J. Engineering a gold-specific regulon for cell-based visual detection and recovery of gold. *Chem. Sci.* 2012, *3* (6), 1780−1784.
(41) Bae, W.; Chen, W.; Mulchandani, A.; Mehra, R. K. Enhanced bioaccumulation of heavy metals by bacterial cells displaying synthetic phytochelatins. *Biotechnol. Bioeng.* 2000, *70* (5), 518−24.
(42) Takahashi, Y.; Kondo, K.; Miyaji, A.; Watanabe, Y.; Fan, Q.; Honma, T.; Tanaka, K. Recovery and Separation of Rare Earth Elements Using Salmon Milt. *PLoS One* 2014, *9* (12), e114858.
(43) Kano, N.; Pang, M.; Deng, Y.; Imaizumi, H. Adsorption of Rare Earth Elements (REEs) onto Activated Carbon Modified with Potassium Permanganate (KMnO4). *J. Appl. Solution Chem. Model.* 2017, *6*, 51−61.
(44) Marwani, H. M.; Albishri, H. M.; Jalal, T. A.; Soliman, E. M. Study of isotherm and kinetic models of lanthanum adsorption on activated carbon loaded with recently synthesized Schiff's base. *Arabian J. Chem.* 2017, *10*, S1032−S1040.
(45) Florek, J.; Mushtaq, A.; Lariviere, D.; Cantin, G.; Fontaine, F.- G.; Kleitz, F. Selective recovery of rare earth elements using chelating ligands grafted on mesoporous surfaces. *RSC Adv.* 2015, *5* (126), 103782−103789.
(46) Kronholm, B.; Anderson, C. G.; Taylor, P. R. A Primer on Hydrometallurgical Rare Earth Separations. *JOM* 2013, *65* (10), 1321−1326.
(47) Franz, K. J.; Nitz, M.; Imperiali, B. Lanthanide-binding tags as versatile protein coexpression probes. *ChemBioChem* 2003, *4* (4), 265−71.


DOI: 10.1021/acs.est.7b02414
*Environ. Sci. Technol.* 2017, 51, 13471−13480

(48) Haas, K. L.; Franz, K. J. Application of Metal Coordination Chemistry To Explore and Manipulate Cell Biology. *Chem. Rev.* 2009, *109* (10), 4921−4960.

(49) spaceTrent, M. S.; Ribeiro, A. A.; Doerrler, W. T.; Lin, S.; Cotter, R. J.; Raetz, C. R. Accumulation of a polyisoprene-linked amino sugar in polymyxin-resistant *Salmonella typhimurium* and *Escherichia coli*: structural characterization and transfer to lipid A in the periplasm. *J. Biol. Chem.* 2001, *276* (46), 43132−44.

(50) Herrera, C. M.; Hankins, J. V.; Trent, M. S. Activation of PmrA inhibits LpxT-dependent phosphorylation of lipid A promoting resistance to antimicrobial peptides. *Mol. Microbiol.* 2010, *76* (6), 1444−60.

(51) Kato, A.; Chen, H. D.; Latifi, T.; Groisman, E. A. Reciprocal control between a bacterium's regulatory system and the modification status of its lipopolysaccharide. *Mol. Cell* 2012, *47* (6), 897−908.

(52) Takahashi, Y.; Yamamoto, M.; Yamamoto, Y.; Tanaka, K. EXAFS study on the cause of enrichment of heavy REEs on bacterial cell surfaces. *Geochim. Cosmochim. Acta* 2010, *74* (19), 5443−5462.

(53) Ngwenya, B. T.; Magennis, M.; Olive, V.; Mosselmans, J. F. W.; Ellam, R. M. Discrete Site Surface Complexation Constants for Lanthanide Adsorption to Bacteria As Determined by Experiments and Linear Free Energy Relationships. *Environ. Sci. Technol.* 2010, *44* (2), 650−656.

(54) Shannon, R. Revised effective ionic radii and systematic studies of interatomic distances in halides and chalcogenides. *Acta Crystallogr., Sect. A: Cryst. Phys., Diffr., Theor. Gen. Crystallogr.* 1976, *32* (5), 751− 767.

## EDITOR'S NOTE

Following acceptance and publication of this article as a Just Accepted Manuscript, Dr. Philip Hageman, with the agreement of all co-authors, was removed as an author; his contribution to the paper was making available samples and giving some advice on methods, which does not constitute a significant scientific contribution.



DOI: 10.1021/acs.est.7b02414
*Environ. Sci. Technol.* 2017, 51, 13471−13480